Petroleum and Coal

Article **Open Access**

Comparison of Well Test Data with Reservoir Data Obtained by Well-Log, Using Well Test Software's and Presenting an Accurate Model According to Both Analytical Solution and Artificial Neural Network for Horizontal Wells in Naturally Fractured Reservoirs

Abbas Ayatizadeh Tanha[1,2], Ghassem Zargar [1,3,] , Mehrshad Mansouri [4], Mehdi Rahmati[1]*

[1] *Ahwaz Faculty of Engineering, Petroleum University of Technology, Iran*
[2] *National Iranian Drilling Company, Well Logging Department, Ahwaz, Iran*
[3] *Faculty Member of Petroleum University of Technology, Iran*
[4] *Institute of Petroleum Engineering (IPE), College of Engineering, University of Tehran, Iran*

Received September 6, 2021; Accepted January 10, 2022

Abstract

Well test analysis is a method for evaluating the average properties of the reservoir by characterizing the ability of the fluid to flow through the reservoir and to the well. Well test output parameters that descript reservoir are permeability, reservoir heterogeneities, boundaries and pressure; also, parameters that descript well are skin factor, productivity index and well geometries. The suggested models for prediction of pressure drop in vertical well have obtained from the solution of diffusivity equation for radial and elliptical regime. The purpose of this project is to generate a model for the horizontal well in fracture reservoir and estimate a parameter for this type of well by ANN method and compare the results with well test software. In this study, pressure data versus time was obtained for horizontal wells in naturally fractured reservoirs by solving diffusivity Equation using Stehfest algorithm, and for each set of data, a polynomial was developed for pressure derivative data by applying Chebyshev polynomials method. The polynomial coefficients along with reservoir and horizontal well data were fed into Artificial Neural Network (ANN) as input data and as a result, a model was presented for the horizontal well in naturally-fractured reservoir. In addition, output of the model was compared to the well log and well test software's data and it was found that the presented model has better and higher performance than well test software's.

Keywords*: Well test; Horizontal well; Naturally-fractured reservoir; Diffusivity equation; ANN method.*

1. Introduction

In recent years, there has been growing interest in neural networks, in which the human brain functions differently than conventional digital computers when it comes to processing information. Neural networks can assist in integration of various types of data in reservoir managing and address both fundamental and specific petroleum engineering problems which conventional calculating has been unable to solve. When required data for modeling and interpretation is insufficient, petroleum engineers can benefit from neural networks.

Hydrocarbon reservoirs are heterogeneous, complex media with characteristics which are generally calculated indirectly by well-testing methods. The well test analysis is basically performed by causing flow disturbances in the well and then measuring the bottom-hole pressure response. This method provides the necessary data for quantitative analyzing the reservoir characteristics and reservoir description. The well-testing technique includes two steps: (1) Recognizing the reservoir model, and (2) estimating the parameters.

The goal of this work is to use the Artificial Neural Network (ANN) in order for reservoir parameters estimation. The applied neural network has a multi-layer perceptron (MLP) structure. The needed training and well test data sets have been developed by using the analytical solutions from common reservoir models. ANN applies input and output data in order to

achieve a relation between them, and unlike symmetric methods, gets its strength from a heavily parallel distributed structure and generalization in which it learns the structure instead of storing information [1].

The following are some of the advantages of ANN to identify reservoir models and evaluate their parameters: (1) Unlike symbolic methods, it has no need to preprocess or write complex rules; (2) it is insensitive to noisy pressure data; and (3) it performs nonlinear mapping for nonlinear issues.

The first use of ANN in well test dates back to the 1990s, when Al-Kaabi and Lee (1990) utilized it to recognize well test models [2]. They applied normalized pressure derivatives in a logarithmic plot as an input to ANN and presented the application of a new artificial neural network-based approach to automatically classify a preliminary well test interpretation model for horizontal wells from the derivative plot and normalized pressure derivative results.

Allian and Houze applied the ANN technique in combination with symbolic approach in their research [3-4]. They used the artificial neural network to recognize the reservoir model type and a symbolic approach to measure parameters of the reservoir.

Although numerous researchers have applied ANN to recognize reservoir models by using data from well test , researches on applying ANN for reservoir parameters estimation are limited [5]

There are three popular techniques for estimating the reservoir parameters from well test data: conventional method, using type-curves, and non-linear regression [5].

In conventional analysis, each flow pattern needs to be plotted individually to estimate reservoir parameters. Therefore, achieving reservoir parameters from all well test data is impossible using this method. In type-curves and nonlinear regression techniques, all the test data are used for reservoir parameters estimation though each approach has its own difficulties. In type-curves, numerous curves may match the pressure data and the results are not unique. On the other hand, because nonlinear regressions are extremely dependent on initial guesses, different results may be obtained from different initial guesses [5].

Drilling horizontal wells has become increasingly more common around the world due to their large contact area with reservoir rock and increased productivity. Horizontal wells provide a very high desired production enhancement as a method for improving production performance [6]. Transient well testing in horizontal oil wells demonstrates more complex behaviors in characterizing reservoir properties when compared to vertical oil wells. The complexity results from the fact that most horizontal wells are not completely horizontal and parallel to the bedding plane. In addition, the wells may be located in the middle of the reservoir thickness, close to the bottom boundary, or close to the top boundary, which affects the flow behavior and makes the interpretation more difficult. Well length, formation thickness, and the ratio of vertical/horizontal permeability are three key parameters that affect transient well tests in horizontal wells [7]. Houzé *et al.* considered the well to be completely horizontal, and to be located in a homogeneous formation of uniform thickness h. First, the reservoir is assumed isotropic in the horizontal plane, but vertical anisotropy and other parameters will be defined as in the limited entry well [8].

Nowadays, naturally fractured reservoirs may comprise a significant portion of total oil and gas production. There are numerous ways to describe this behavior; however, the purpose of this study is to use pressure transient tests in a horizontal well in order to better understand and describe these types of reservoirs [9]. The ultimate goal is to accurately characterize the reservoir properties, like skin factor, permeability and storage capacity of each medium [10]. In the following, the core theory of this study is presented. The data set and methodology are discussed in Section 3. This is followed in Section 4 by presentation and discussion of the results obtained.

2. Theory

Due to the properties of noise insensitive and nonlinear mapping, ANN has been widely used to solve nonlinear problems in recent years. The ANN training samples are a series of data points taken from theoretical pressure derivative curves. The data point series is normalized or scaled down to [0, 1] or [−1, 1] before input to ANN to uniform the input data and

prevent saturation while training ANN [11]. Since actual tested pressure derivative curves are unavailable as learning samples to train ANN due to the complexity of the well test problem, the logical training samples are the theory pressure derivative curves based on the mathematical model. In comparison to the training samples, the actual tested pressure derivative curve is normally transferred, noised, and truncated, resulting in the tested curve not being in the same model area as the training samples [12-13].

Using ANN for reservoir characteristics estimation of Naturally Fractured Reservoirs (NFRs) was conducted by Alajmi and Ertekin (2007) for first time [?]. They obtained a coefficient of interpolating polynomials by fitting a conventional polynomial of degree 4 to pressure data plotted in a semi-log scale and applied this coefficient as input of the ANN.

Serra et al. showed that three different semi-log flow patterns can be observed for pressure responses of naturally fractured reservoir, and they also provided methods to classify these flow regimes using field data, as well as the times and physical conditions under which they occur [14]. Using the pressure curves plotted in the semi-log format to train the ANN, is the main drawback of their work. These curves, when compared to the pressure derivative data plotted in log–log format, are extremely similar for NFRs to effectively conduct the learning process, and consequently, learning process of the ANN discovered to be very tedious [15-16].

In this study, Pressure derivative data in the log–log scale is applied to train the ANN. The fundamental concept is to fit a polynomial to pressure derivative data in a log–log format and use the interpolating polynomial coefficient as an input to the ANN instead of normalized data. Also, Chebyshev polynomials were applied to interpolate the pressure derivative data. Furthermore, a reservoir model which corresponds to NFR with PSS inter-porosity flow is used and all unknown reservoir parameters are determined using ANN. These parameters are as following: (1) wellbore storage(C); (2) skin (S); (3) permeability of fracture (kf); (4) inter-porosity flow coefficient (λ); (5) storativity ratio (ω) [17].

3. Data Set

General description

The oilfield illustrated in Figure 1 is the largest onshore oilfield discovered in the last three decades and is located in south-west of Iran. Sarvak, Kazhdumi, and Gadvan are productive reservoirs of this field [18].

Figure 1. Regional location map of A specific oil field in southwest Iran

Well information

The exploration and delineation drilling in this field has proved presence of a very prolific hydrocarbon-enriched bearing sedimentary column.

Fracturing

Fracturing affects all rock types and can increase reservoir potential. Vugs developed in Middle Sarvak with vertical variations can be observed in outcrops at different scales in Bangestan (about 200 kilometers west of this oilfield). Figure 2 shows developed and undeveloped vugs in Sarvak outcrops [6].

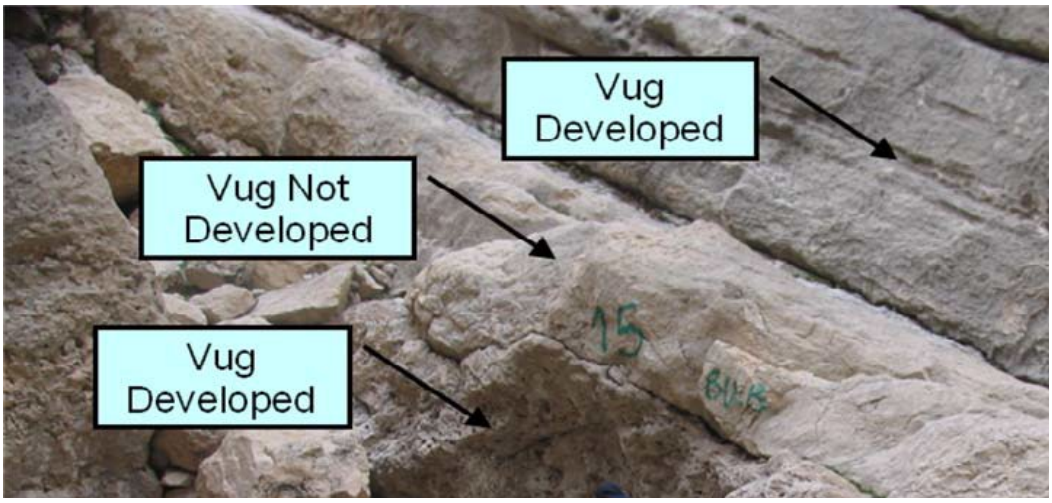

Figure 2. Developed Vugs in Bangestan

In order to investigate the correlation between lithological data and reservoir properties graphically, comprehensive reservoir columns are generated by using lithological, core porosity and permeability, in addition to log data, as shown in Figure 3.

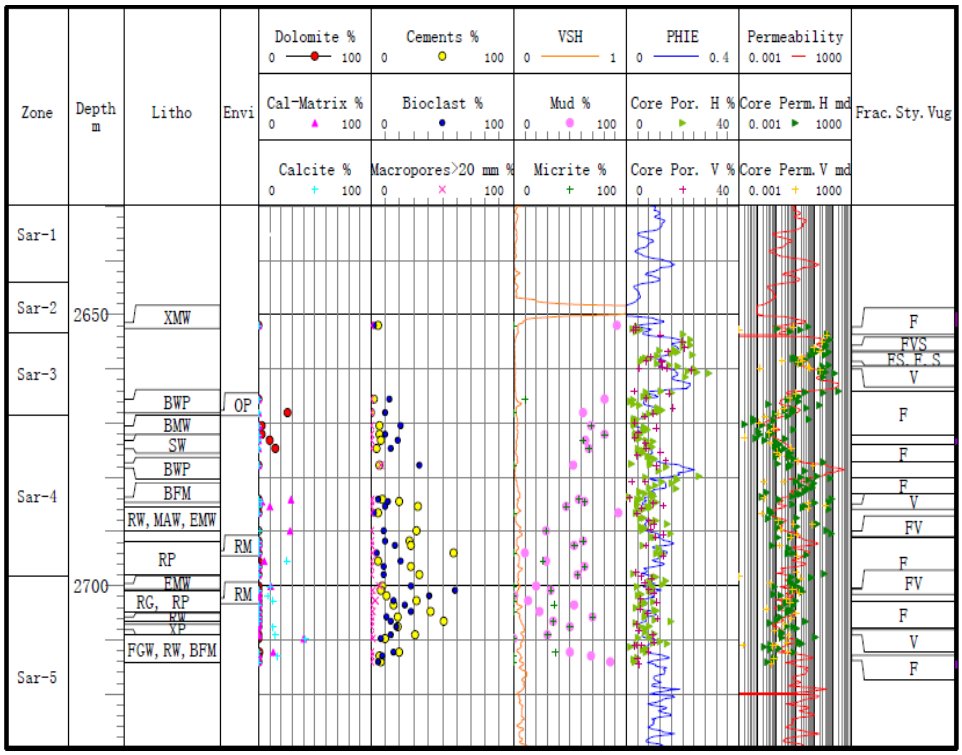

Figure 3. Comprehensive reservoir column of Well-A

Fractures in Sarvak

Due to the lack of FMI and outcrop data, there is no direct evidence of fracture distribution. However, the existence of fractures is confirmed by the following indirect evidences:

1. Some cores are fragmented and have stylolite-related micro fractures.

Figure 4. Well-A core photograph

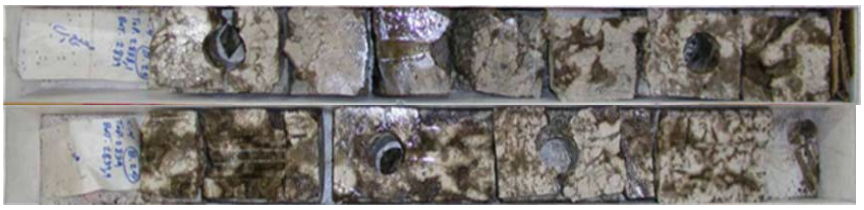

Figure 5. Well-B core photograph

2. The results of a plug permeability analysis show values as high as 1256 md, which could be an indication of fracture. The values of permeability can be found in Table 1; and the corresponding logs are illustrated in Figure 6. Also, the mercury injection curves of Well-A at 2756 m are displayed in Figure 7.
3. Reservoir properties and well test results in the oilfield have been recorded in Tables 2 and 3 respectively. As it can be observed, Sarvak is a low-permeability reservoir with an average permeability of 11.6 md which has been measured from log interpretation. However, the high production test (over 6000 bbl/d in Well-C) of some wells is inconsistent with the low permeability of this layer. This productivity can result from the existence of fractures.
4. Fracture Analysis of Well-A: EMI logging was conducted in Well-A. Analysis shows that (1) Conductive fractures are generally not formed, with only 8 fractures identified; (2) resistive fractures are also not developed, with only 2 fractures identified; and (3) one group of induced fractures is found with a high dip angle, which may be linked to the release of geostress.

Table 1. Permeability of core in Well-A

Well	Sample	Zone	Core depth(m)	MD (m)	Porosity	Permeability
Well-A	2-2	Sar-3	2756.4	2759.9	0.101	1256
Well-A	2-6	Sar-3	2765.4	2768.9	0.236	89
Well-A	2-10	Sar-3	2774.1	2775.7	0.208	29
Well-A	2-22	Sar-3	2871.1	2873.8	0.039	0.69

Table 2. Reservoir properties of the Specific oilfield

Form.	Net	k	μ	Kh/μ	GOR	B_{oi}	P_i-P_b
Sar.	75.2	11.6	5	174	267 - 493	1.25-1.35	2700 - 3629
Kaz.	10.8	99.1	0.4	2696	916 - 1589	1.38 - 1.95	1299 - 2689
Gad.	13.3	181.5	0.35	6897	1168 - 1391	1.79 – 1.87	2277 - 2933
Fah.	36.2	11.5	0.33	913	1519 - 1996	1.8 – 2.08	4710 - 5400

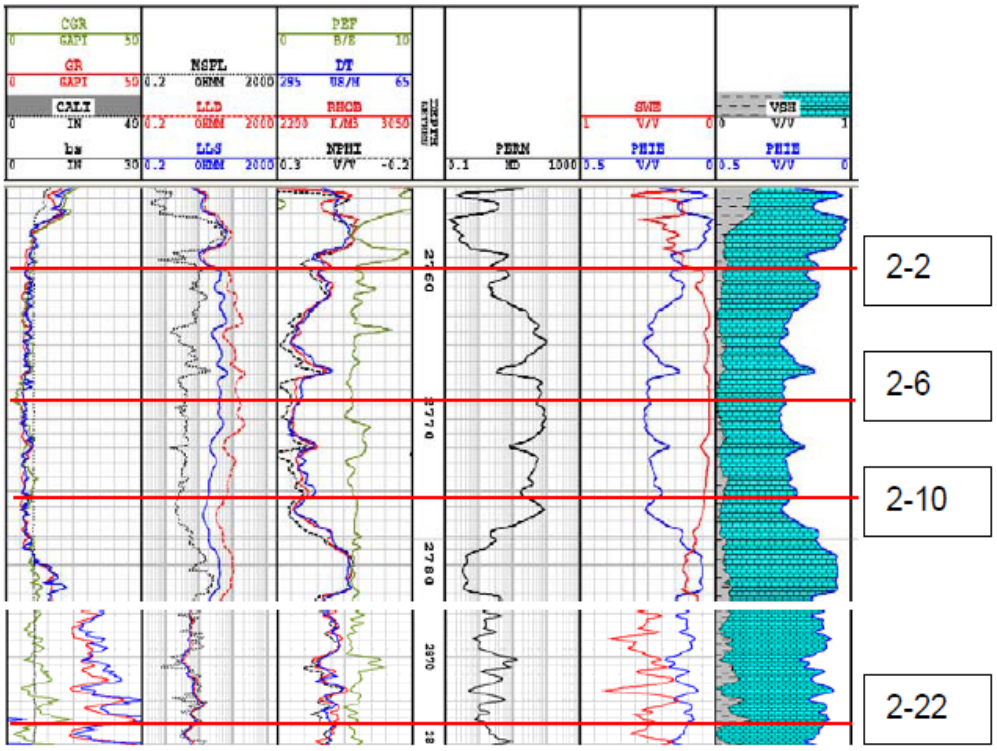

Figure 6. Logging depth and features for samples in Table 1

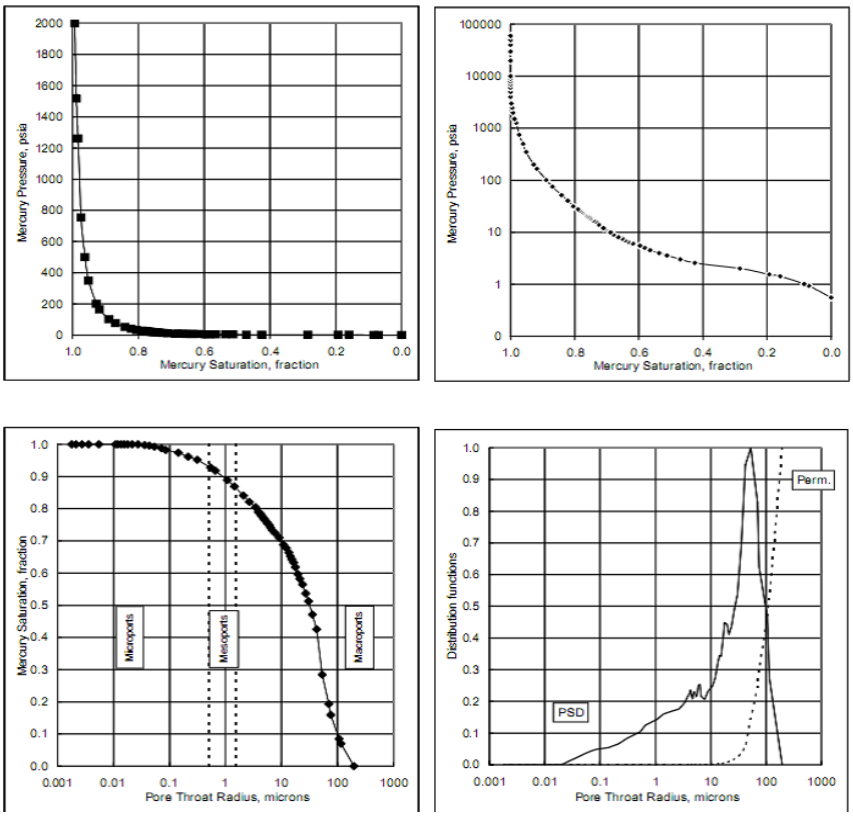

Figure 7. Mercury injection data of 2-2 sampled in Well-A well

Table 3. Well test result

Well	Test.no	Top depth	Base depth	Pressure	Oil (bbl/D)	Gas	Oil gas
Well-B	PT1	2800	2820		335-425		1020
Well-B	PT2	2762	2778	469	4602		1571
Well-C	PT2	2930	2953	0-70			
Well-C	PT3	2928	2938	50-60	706		2436
Well-C	PT4	2806	2821	810	6238	197	290
Well-C				1030	4260	108	290
Well-C				1200	1902	126	290

Methodology

Artificial Neural Network of which the specification has been reported in Table 4, is applied to evaluate reservoir parameters using data from well test. The Stehfest numerical Laplace inverse algorithm was employed to train the ANN on theoretical pressure derivative curves from a NFR with Pseudo Steady State (PSS) inert porosity flow in a horizontal well [19].

Table 4. Initial and steady states values of output

ANN				
Hidden layer transfer function	Output layer transfer function	Number of neurons in input layer	Number of neurons in hidden layer	Number of neurons in output layer
sigmoid	linear	17	15	8

Each reservoir parameter is estimated using all test data for verification of the accuracy of the trained ANN. The ability of the new method, which uses curve fitting polynomial coefficients as input to train ANN, is demonstrated by low relative error values of reservoir parameters when test data is used. Furthermore, well test data for a fractured reservoir with dual-porosity model in a horizontal well in this oil-field was used to compare the outputs of the ANN with the results achieved using various well test software's and normalization methods. The results indicate that ANN and well test software's are very consistent [20-22].

The pressure derivative data plotted in log-log scale are obviously more recognizable compared to the pressure drop data in a semi-log format. Even by using different reservoir parameters, the similarity of the pressure data in a semi-log scale leads to the same input data for ANN, which causes difficulties in the learning process. Due to the problems with normalized input data, a new approach is presented in this study to explain the properties of pressure derivative data used as an input to the ANN.

The main idea is to fit a polynomial to pressure derivative data in a log–log plot and use the interpolating polynomial coefficients as inputs to the ANN instead of normalized data. The main issue, however, is that the pressure derivative curves of NFRs in horizontal wells are extremely dissimilar for different values of λ, ω, Lw, or so. As a result, higher order polynomials are required. Figure 8 shows simulations of pressure derivative data plotted in log–log format for different parameters.

A polynomial fit was created to effectively preserve the signature integrity of the double porosity model in horizontal well. This procedure necessitates the use of the following curve fitting tool box of Matlab software. Quantitative data can be fully utilized by fitting the data to a mathematical model.

It was observed that a suitable polynomial of degree nine produced a very good fitting between the polynomial and the pressure transient data. As a result, the ten characteristic polynomial coefficients are used to replace the data point pressure transient data, which effectively explain the double porosity in each pattern's horizontal well signature. The use of the polynomial fit procedure has been displayed in Figure 9. Also, an example of the obtained polynomial coefficient by using the polynomial fit algorithm has been recorded in Table 5 [23].

$$f(x) = p_1x^9 + p_2x^8 + p_3x^7 + p_4x^6 + p_5x^5 + p_6x^4 + p_7x^3 + p_8x^2 + p_9\,x + p_{10} \quad (1)$$

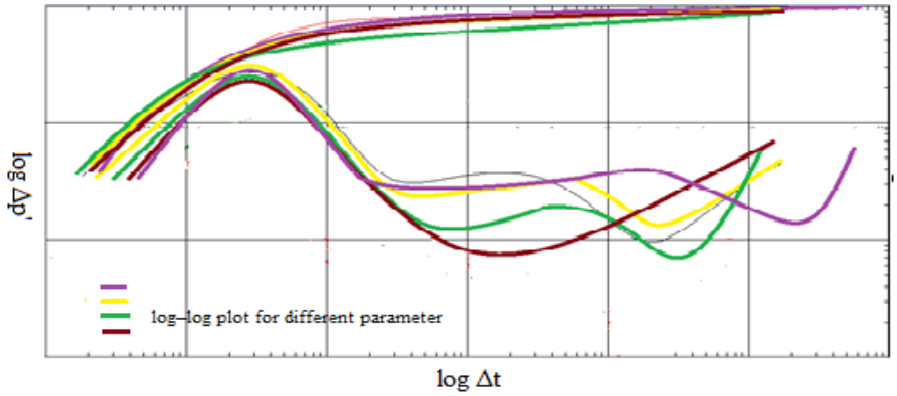

Figure 8. Simulated logΔP' vs. Δt for different parameters

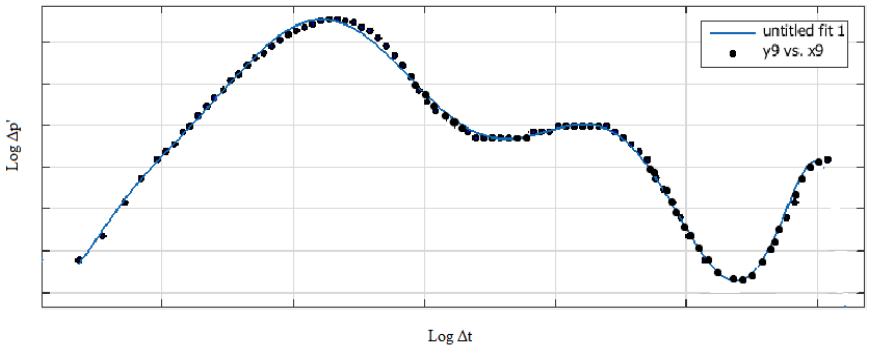

Figure 9. A polynomial fiting procedure demonstration

Table 5. An example of the obtained polynomial coefficient using the polynomial fit algorithm

Polynomial coefficient	Value
P_1	-0.2127
P_2	-0.5372
P_3	1.161
P_4	3.394
P_5	-1.73
P_6	-6.748
P_7	0.8511
P_8	3.856
P_9	-1.134
P_{10}	-6.574

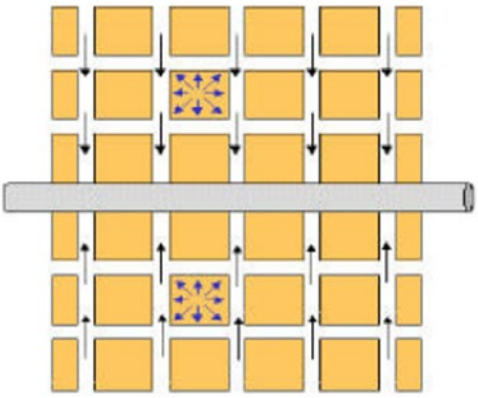

Figure 10. Horizontal well schematic in dual-porosity and single permeability reservoir [24]

Pressure behavior of horizontal wells in natural fractured reservoirs

In horizontal wells in NFRs, the Warren and Root model, a dual-porosity and single-permeability model, is used in each pressure drawdown and buildup equation. This study presents an analytical solution for pressure transient behavior of a horizontal well in dual-porosity, dual-permeability NFRs. When we consider the flow condition inside the matrix blocks, the proposed equations can be derived using the double Fourier transform and Laplace transformation. The

results measured for combinations of dimensionless characterization parameters, like permeability ratio between matrix and fracture structures, have shown the unique behavior of NFRs. [24].

Model of horizontal well

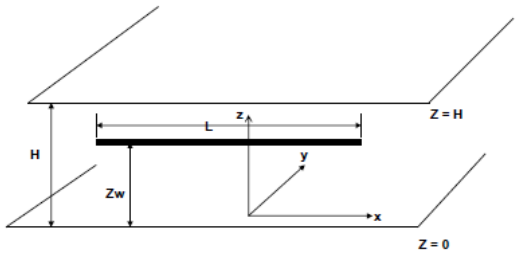

Figure 11. Horizontal well configuration

Figure 11 shows a schematic of a horizontal well with length L which is parallel to x direction. The following assumptions have been considered:

1. The dual-porosity NFR is a horizontal layer of which thickness, porosity, and permeability's of matrix and fracture are constant.
2. The matrix system is homogeneous and isotropic, as is the fracture system.
3. Since the reservoir has an infinite lateral extension, pressure disturbances during well production do not reach the boundaries.
4. The initial pressure in the reservoir is constant, and it is uniform in the reservoir. At an infinite distance from the well, the pressure remains constant and equal to the initial value. The reservoir is also bounded by top and bottom impermeable layers.
5. The production takes place through a horizontal well with a radius of r_w and a length of L, which is illustrated in the model by a uniform line sink located at a distance of w z from the lower boundary. In addition, the formation's thickness is small in comparison with the horizontal well's length.
6. A single-phase fluid with a low and constant compressibility C, constant viscosity μ, and formation volume factor B_o enters from the reservoir to the well. Also, flow rate is Constant and Fluid properties are pressure-independent.
7. Interporosity flow between the matrix blocks and fractures occurs in a pseudo-steady state, and both the fracture system and the matrix blocks will feed the horizontal wellbore.
8. The effect of gravity drainage is ignored.

Initial and boundary conditions

As it can be observed in Figure 11, the horizontal well is a uniform line sink in 3 dimensions, and the coordinates of the 2 ends are (0, 0, z_w) and (L, 0, z_w). The drainage domain is:

$$\Omega\ (-\infty, \infty) * (-\infty, \infty) * (0, H) \quad (2)$$

The reservoir is infinite laterally extended; it means that the outer boundary condition is as follows:

$$P_j\ (r, t) = P_{ini};\ \text{when } r \to \infty\ ;(\ j = 1, 2) \quad (3)$$

where P_{ini} is the initial pressure in the reservoir, and subscripts 1 and 2 respectively denote the matrix block structure and the fracture system. In addition, upper and lower boundaries of the reservoir are impermeable.

$$\frac{\partial pj}{\partial z}|z = o = \frac{\partial pj}{\partial z}|z = H = 0;(\ j = 1, 2) \quad (4)$$

Boundary condition at wellbore:

$$P_1\ (r_w, t) = P_2\ (r_w, t) = P_w\ (t) \quad (5)$$

Initial condition: $P_j\ (r, t) = P_{ini}$; when t=0 ;(j = 1, 2)

At each mathematical point, the medium and flow parameters of both fracture and matrix media are described using continuum mechanics. The pressure equations for a single point sink are obtained, and then the solutions for a uniform line sink are obtained using the principle of superposition [25-26].

Point Sink Solution

In the dual-porosity, and dual-permeability NFRs, let the system of equations for a point sink at (x', 0, z_w) be as follows:

$$\frac{\partial^2 P_m}{\partial x^2}+\frac{\partial^2 P_m}{\partial y^2}+\frac{\partial^2 P_m}{\partial z^2}+\alpha(P_f-P_m)=\left(\frac{\mu\varphi_m C_m}{K_m}\right)\frac{\partial P_m}{\partial t}+\left(\frac{\mu B_o q_m}{K_m}\right)\delta(x-x')\delta(y)\delta(z-z_w) \quad (6)$$

$$\frac{\partial^2 P_f}{\partial x^2}+\frac{\partial^2 P_f}{\partial y^2}+\frac{\partial^2 P_f}{\partial z^2}+\left(\frac{K_m\alpha}{K_f}\right)(P_m-P_f)=\left(\frac{\mu\varphi_f C_f}{K_f}\right)\frac{\partial P_f}{\partial t}+\left(\frac{\mu B_o q_f}{K_f}\right)\delta(x-x')\delta(y)\delta(z-z_w) \quad (7)$$

The ratio of matrix permeability to fracture permeability is defined in the equation below:

$$D=\left(\frac{K_m}{K_f}\right) \quad (8)$$

$$\beta=\frac{D}{(1+D)} \quad (9)$$

Assume q_m is the flow rate of matrix block system, and q_f is the flow rate of fracture system, then we can obtain the total flow rate of horizontal well, q_w:

$$q_w = q_m + q_f \quad (10)$$

Define:

$$\tau_m=\frac{q_m}{q_w} \quad (11)$$

$$\tau_f=\frac{q_f}{q_w} \quad (12)$$

And assume:

$$\tau_m=\frac{k_m}{k_f+k_m} \quad (13)$$

$$\tau_f=\frac{k_f}{k_f+k_m} \quad (14)$$

Then:

$$q_m=\frac{k_m q_w}{k_f+k_m}=\tau_m q_w \quad (15)$$

$$q_f=\frac{k_f q_w}{k_f+k_m}=\tau_f q_w \quad (16)$$

The storage capacity ratio is calculated as follows:

$$\omega=\frac{\varphi_f C_f}{(\varphi_m C_m+\varphi_f C_f)} \quad (17)$$

The interporosity flow parameter is:

$$\lambda=\frac{\alpha k_m h^2}{k_f+k_m} \quad (18)$$

Using dimensionless transformations, Equations (6) and (7) are changed to:

$$\beta\left(\frac{\partial^2 P_{dm}}{\partial x_d^2}+\frac{\partial^2 P_{dm}}{\partial y_d^2}+\frac{\partial^2 P_{dm}}{\partial z_d^2}\right)+\lambda(P_{df}-P_{dm})=(1-\omega)\frac{\partial P_{dm}}{\partial t_d}-\tau_m\delta(x_d-x'_d)\delta(y_d)\delta(z_d-z_{dw}) \quad (19)$$

$$(1-\beta)\left(\frac{\partial^2 P_{df}}{\partial x_d^2}+\frac{\partial^2 P_{df}}{\partial y_d^2}+\frac{\partial^2 P_{df}}{\partial z_d^2}\right)-\lambda(P_{df}-P_{dm})=\omega\frac{\partial P_{df}}{\partial t_d}-\tau_f\delta(x_d-x'_d)\delta(y_d)\delta(z_d-z_{dw}) \quad (20)$$

Then, we can attain the point sink solution at (x_d' ,0, z_{wd}) using the Laplace transform and double Fourier transform of Equations (19) and (20), along with boundary and initial conditions:

$$p_{df}(x'_d,z_{wd},t_d)=-\sum_{n=0}^{\infty}\cos\left(\frac{n\pi z_{wd}}{h_d}\right)\cos\left(\frac{n\pi z_{wd}}{h_d}\right)\times\left[\tau_m f_{3,n}(\beta,\lambda,\omega,x_d,y_d,x'_d,t_d)+\tau_f f_{4,n}(\beta,\lambda,\omega,x_d,y_d,x'_d,t_d)\right] \quad (21)$$

Where:

$$f_{j,n}(\beta,\lambda,\omega,x_d,y_d,x'_d,t_d)=\left(\frac{1}{2\pi}\right)\int_{-\infty}^{\infty}\int_{-\infty}^{\infty}F_{j,n}(\beta,\lambda,\omega,\gamma,x'_d,t_d,\xi_1,\xi_2)\exp[i(\xi_1 x_d+\xi_2 y_d)]\,d\xi_1 d\xi_2 \quad (22)$$

And: $F_{3,n}(\beta,\lambda,\omega,\gamma,x'_d,t_d,\xi_1,\xi_2)=\left[\frac{exp(-i\xi_1 x'_d)}{2\pi h_d d_n}\times\left\{\left[\frac{\lambda}{\omega(\omega-1)}\right]\times\left[\frac{(a-b)+b\,exp(at_d)-a\,exp(bt_d)}{ab(a-b)}\right]\right\}\right]$ (23) (24)

In above equation:

$$a=\frac{(-U+\sqrt{U^2-4V})}{2}$$

$$F_{4,n}(\beta,\lambda,\omega,\gamma,x'_d,t_d,\xi_1,\xi_2)=\left[\frac{\exp(-i\xi_1 x'_d)}{2\pi h_d d_n}\times\left\{\left[\frac{\beta\gamma^2+\lambda}{\omega(\omega-1)}\right]\times\left[\frac{(a-b)+b\exp(at_d)-a\exp(bt_d)}{ab(a-b)}\right]-\left(\frac{1}{\omega}\right)\times\left[\frac{\exp(at_d)-\exp(bt_d)}{a-b}\right]\right\}\right]$$

(25)

$$b = \frac{(-U-\sqrt{U^2-4V})}{2} \quad (26)$$

$$U = \frac{(-2\beta\omega\gamma^2-\gamma^2+\beta\gamma^2-\lambda+\omega\gamma^2)}{-\omega+\omega^2} \quad (27)$$

$$V = \frac{(-\beta\gamma^4-\lambda\gamma^2+\beta^2\gamma^4)}{-\omega+\omega^2} \quad (28)$$

$$\gamma^2 = {\xi_1}^2 + {\xi_2}^2 + \left(\frac{n\pi}{h_d}\right)^2 \quad (29)$$

Uniform line sink solution

By assuming the horizontal well as a uniform line sink, located between points (0,0, z_w) and (L,0, z_w), and dimensionless line sink locating between points (0,0,z_{wd}) and (L_d,0, z_{wd}), the dimensionless pressure at the wellbore point (x_d ,0,z_{wd}) is as the following, by using Principle of Superposition, and recall Equation (5):

$$p_{wd}(x_d, x'_d, z_{wd}, t_d) = -\sum_{n=0}^{\infty} cos\left(\frac{n\pi_d}{h_d}\right) cos\left(\frac{n\pi_{wd}}{h_d}\right) \times \left[\tau_m g_{3,n}(\beta, \lambda, \omega, x_d, y_d, x'_d, t_d) + \tau_f g_{4,n}(\beta, \lambda, \omega, x_d, y_d, x'_d, t_d)\right] \quad (30)$$

where:

$$g_{j,n}(\beta, \lambda, \omega, x_d, y_d, x'_d, t_d) = \int_0^{l_d} f_{j,n}(\beta, \lambda, \omega, x_d, y_d, x'_d, t_d)\, dx'_d \quad (31)$$

Equation (4.22) for all h > 0 will change to:

$$\int_{-\infty}^{\infty}\int_{-\infty}^{\infty} F(\xi_1, \xi_2) d\,\xi_1 d\xi_2 = \sum_{i=-\infty}^{\infty}\sum_{m=-\infty}^{\infty}\int_{ih}^{(i+1)h}\int_{mh}^{(m+1)h} F(\xi_1, \xi_2) d\,\xi_1 d\xi_2 \quad (32)$$

Then by applying Mean Value Theorem, we obtain:

$$f_{j,n}(x_d, y_d) = \left(\frac{1}{2\pi}\right)\sum_{i=-20}^{20}\sum_{m=-20}^{20} h^2 F_{j,n}\left[\left(i+\frac{1}{2}\right)h, \left(m+\frac{1}{2}\right)h\right], (j = 3,4) \quad (33)$$

At very early time, the horizontal wellbore pressure can be calculated as follows using Equations (30), (31), (32), and (33):

$$p_{wd} = \frac{1}{2}\{1.423 + ln(t_d)\} - \frac{1}{4} ln[4\, sin(\pi z_{wd})\, sin(\pi r_{wd})] \quad (34)$$

where:

$$\chi = \left(\frac{1+D}{D\sqrt{\eta_1}+\sqrt{\eta_2}}\right) \quad (35)$$

and:

$$\eta_1 = \frac{1-\omega}{\beta} \quad (36)$$

$$\eta_2 = \omega(1+D) \quad (37)$$

When t_d < 0.05, L_d> 5, Equation (34) changes to:

$$p_{wd} = \left(\frac{2\chi}{L_d\sqrt{\pi}}\right)\sqrt{t_d} \quad (38)$$

At very late time, if D< 0.25, t_d > 10^3 there holds:

$$p_{wd} = \frac{1}{2}\left\{1.423 + ln(t_d) + Ei\left[\frac{-\lambda t_d}{\omega(1-\omega)}\right] - Ei\left[\frac{-\lambda t_d}{(1-\omega)}\right]\right\} - \frac{1}{4} ln[4\, sin(\pi z_{wd})\, sin(\pi r_{wd})] \quad (39)$$

When t_d > 10^5, Equation (39) reduces to:

$$p_{wd} = \frac{1}{2}\{1.423 + ln(t_d)\} - \frac{1}{4} ln[4\, sin(\pi z_{wd})\, sin(\pi r_{wd})] \quad (40)$$

In oil field units if only the mechanical skin factor is considered, Equation (40) is expressed as follows:

$$p_{ini} - p_w = \left(\frac{162.6\mu B_o q_w}{k_t h}\right)\left\{0.618 + log\left(\frac{k_t t}{\mu(\varphi c)_t h^2}\right) - \left(\frac{h}{L}\right) log\left[4\, sin\left(\frac{\pi z_w}{h}\right) sin\left(\frac{\pi r_w}{h}\right)\right] + 0.217\left(\frac{h}{L}\right) S_m\right\} \quad 41)$$

The Stehfest algorithm is applied to develop pressure derivative data from the pressure solution in Laplace media. By considering the impacts of wellbore storage and skin factor, and also using the above equation (41), the proposed method is utilized to develop the pressure derivative data, which is defined in the following [5, 27, 28]:

$$\xi\left\{\frac{dp_{wd}}{dt_d}\right\} = s\bar{p}_{wd}(s) - p_{wd}(t_d = 0) \quad (42)$$

$$\frac{dp_{wd}}{dt_d} = \xi^{-1}\{s\bar{p}_{wd}(s)\} \quad (43)$$

$$\left(t_d \frac{dp_{wd}}{dt_d}\right)_i = \left(\frac{dp_{wd}}{d\, ln(t_d)}\right)_i = t_{di}[\xi^{-1}\{s\bar{p}_{wd}(s)\}]_{t_{di}} \quad (44)$$

$$\bar{p}_{wd}(s) = \frac{h_d}{2s} k\left\{\sqrt{[x_d^2 + (z_d)^2]sf(s)}\right\} \quad (45)$$

where:

$$f(s) = \omega + \frac{(1-\omega)\lambda}{(1-\omega)s+\lambda} \quad (46)$$

Eq. (4.43) ignores the influence of rock and fluid properties due to the fact that it only generates dimensionless pressure derivative data points. As a result, using the following equations, the dimensionless pressure derivative data and the dimensionless time are changed to the derivative of pressure drop data versus time [5]:

$$\left(t\frac{\delta\Delta p}{\delta t}\right)_i = \frac{141.2q\mu B_o}{k_f h}\left(t_d\frac{\delta p_d}{\delta t_d}\right)_i \quad (47)$$

$$t = \frac{\mu(\phi c_t)_t {r_w}^2}{0.000264k_f} t_d$$

While ANN has been trained applying drawdown pressure derivative curves, the buildup pressure test data can be introduced to ANN using Agarwal's equivalent time, which is defined as follows: [29]

$$t\frac{t_p\Delta t}{t_p+\Delta t}_{sup.} \quad (48)$$

Artificial neural network process

Curve fitting polynomials of degree 9 are applied to interpolate the pressure derivatives time data points, and the corresponding coefficients P_i (i=1-9) are determined using the Least-Square method. These coefficients are then fed into the ANN together with the rock and fluid properties. As it is illustrated in Figure 12, there is an optimal value for the degree of curve fitting polynomials. Low degrees of curve fitting polynomials do not precisely match the pressure derivative data, while greater degrees interpolating polynomials enlarge the number of input data to the ANN without significantly improving the fitting, which in turn, leads to a complicated learning process of ANN.

A one-layer back-propagation (BP) neural network is used after testing different possible configurations of ANN. Therefore, a one-layer ANN was found to be adequate in this case. Minimizing Mean Relative Error (MRE) through which the number of neurons in the first hidden layers was optimized over the test data, is defined as follows [23]:

$$MRE = \frac{1}{N_T}\frac{1}{8}\sum_{i=1}^{8}\sum_{j=1}^{N_T}\frac{|(out_{real})_{i,j}-(out_{net})_{i,j}|}{|(out_{real})_{i,j}|} \quad (49)$$

Where N_T is the number of test samples in the above equation. The upper bound of the first summation has been set to the output parameters of the ANN, which are eight different parameters.

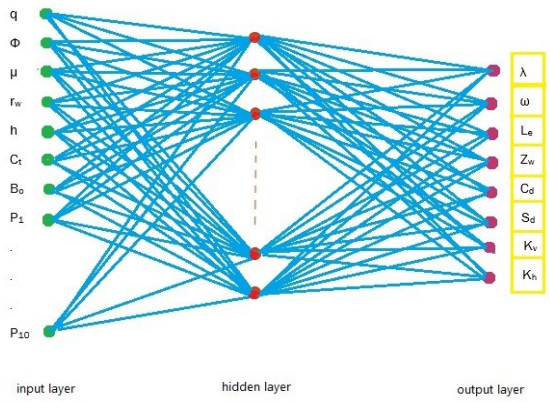

Figure 12. Schematic of the ANN applied to estimate the parameters

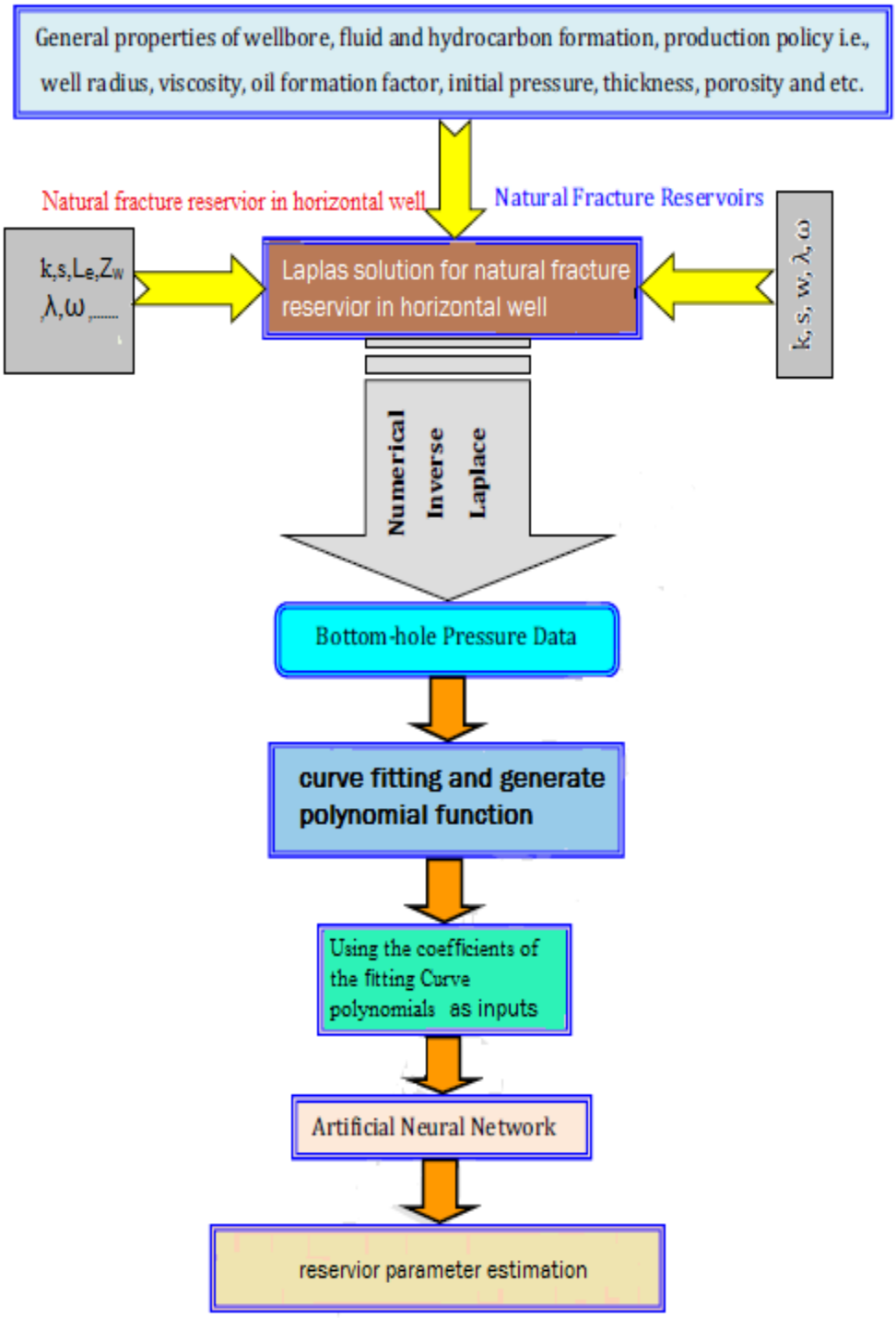

Figure 13. Workflow of the performed analysis for reservoir model detection

4. Results

In this study, in addition to polynomial curve fitting method, other techniques have also been used to analyze well test data. Then, the results will be compared to the new proposed technique. Based on these methods, an interactive computer aided well test interpretation

software has been used of which the results have been compared to actual data in Sarvak formation in The oil field.

In order for accuracy verification of the trained ANN with fitted polynomials, field data which have been derived from drill stem test in The oil field areal were introduced to the ANN in addition to applying relative error over test data. By using these data, the performance of ANN was evaluated in the case of real noisy pressure data.

It is worth noting that this case is a draw down test with flow rate of 400 STBD and production time which is equal to 90 hr. Figure 14 shows flow rate schedule.

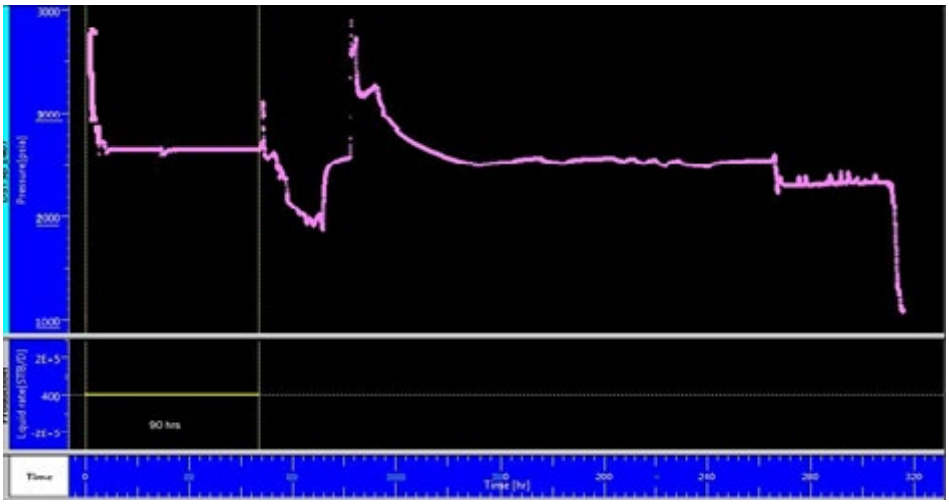

Figure 14. Production history

Fluid and rock data corresponding to this test have been reported in Table 6 and the pressure derivative response during the test has been illustrated in Figure 15.

Table 6. The fluid and rock parameters related to Well-B

q (Rbbl/STB)	μ_o(CP)	Φ_t	r_w(ft)	h(ft)	C_t(1/psi)
400	5	0.2	0.37	247	1.67E-05

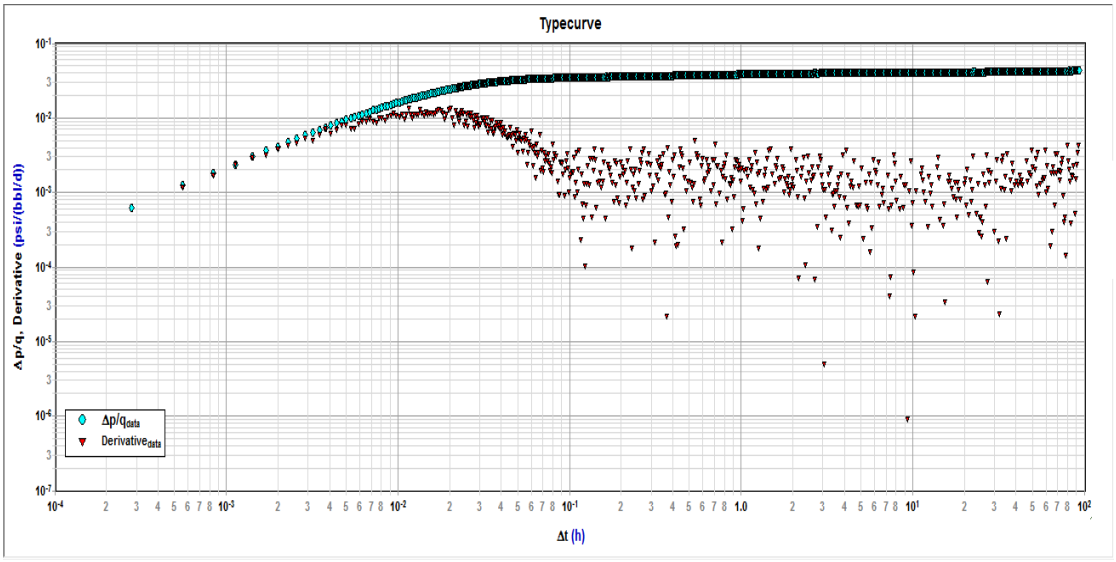

Figure 15. Pressure derivative results during well-testing in Well-B

A deep valley in the pressure derivative response demonstrates truly dual-porosity system of the reservoir and the effect of horizontal well also be shown in figure above. The shape of

the fitting polynomial and matched curve is shown in Figure 16. Also the coefficients of the fitting polynomial are shown in Table 7.

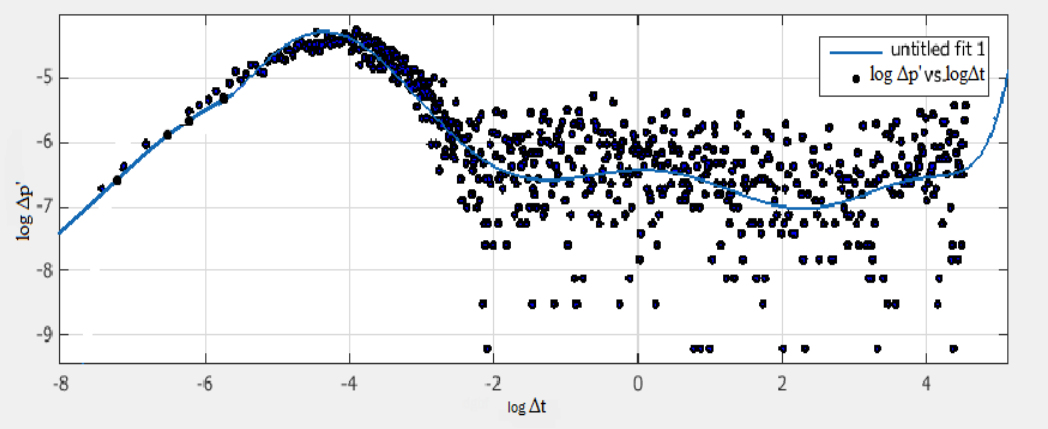

Figure 16. LogΔP' vs. logΔt together with the fitting polynomial of degree 9 for a field case Well-B

Table 7. The fitting polynomial Coefficients for the drawdown test performed in Well-B

Polynomial coefficient	Value	Polynomial coefficient	Value
P1	0.05318	P6	1.748
P2	0.1048	P7	-0.2847
P3	-0.5211	P8	-0.7023
P4	-0.8006	P9	0.4483
P5	1.93	P10	-6.475

Fitting polynomials coefficients of used data were compared to the results of well test software's like Saphir and Fast in order to test the new presented technique. The results corresponding to the ANN by utilizing the fitting polynomial and well test software's are given in Table 8.

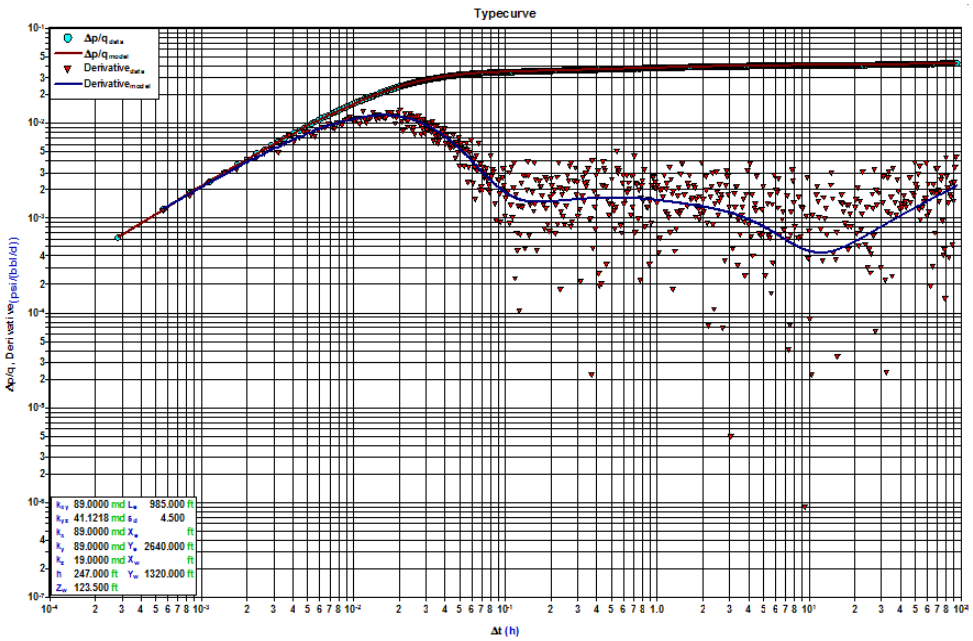

Figure 17. An analysis of pressure and pressure derivative through nonlinear regression for Well-B using Fast

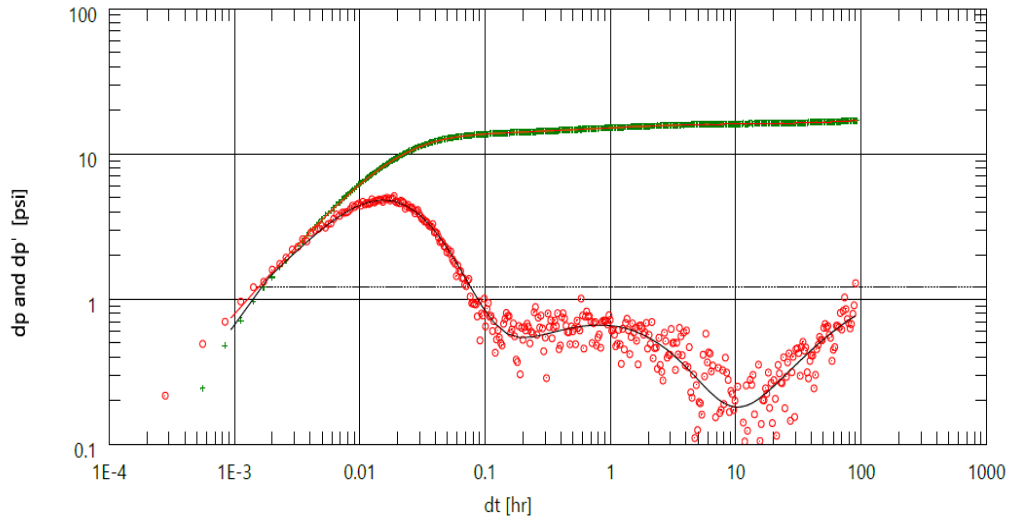

Figure 18. Results of pressure and pressure derivative data through nonlinear regression for Well-B

Table 8. The fitting polynomial coefficients for the drawdown test data performed in Well-B

	Real data	Saphir	Fast	New method
K_v	1259	484	512	954
K_h	89	121	115	93
L_e	1650	1921	2021	1712
Z_w	120	123	145	122
C_d	115	174	148	133
S	*	3.68	4.5	4.52
ω	*	0.0324	0.0301	0.0311
λ	*	2.27E-07	4.57E-07	4.2E-07

As it can be observed in Table 8, the evaluated parameters of the ANN trained by using the fitting polynomials coefficients, lie between those calculated by well test software's and actual data. As a result, the logarithmic pressure derivative curves are represented more accurately through fitting polynomials whereas less input data is fed into the ANN. In other words, using the fitting polynomials as the input data makes the ANN more efficient in comparison with conventional techniques which use pressure derivative data and time as inputs to the ANN.

5. Conclusion

In this study, the fundamentals of analytical pressure transient analysis were represented and draw down test data of a well in Sarvak formation, a very complex fractured reservoir in southwest of Iran, were analyzed by an analytical model and also a numerical model using ANN. The complexity of this formation requires special data analysis techniques. In this work many efforts have been made to accurately analyze pressure draw down tests using two well-known industrial software including 'Saphir' from Kappa Engineering and 'FAST Welltest' from Fekete, Inc.

Based on the analysis of draw down test conducted in a horizontal well and also the new method obtained for parameter estimation in the oilfield, the followings conclusions can be made:

1. Sarvak formation in The oil field has many vugs and fractures which should be considered in similar studies or interpretations.

2. Running ANN model without initial values form analytical model takes a long time to converge and sometimes it may not converge. Therefore, it is recommended to use the final results of analytical model as initial guess for numerical models.
3. By applying the data fitting coefficients as input data to ANN, its learning process has been enhanced.
4. Estimated effective length of horizontal wells has a high value of mean relative error because of drilling problems.

Nomenclature

A	*Total cross section area, ft²*
B	*Formation volume factor*
B_O	*Oil formation volume factor, RB/STB*
B_g	*Gas formation volume factor, RB/MSCF*
C_t	*Total compressibility, 1/psi*
C	*Well bore storage coefficient, RB/psi*
C_D	*Dimension well bore storage coefficient*
h	*Thickness of layer, ft²*
k	*Permeability, md*
p	*Pressure, psi*
p_{1hr}	*Pressure for ⊿t=1hr on the semi-log straight line, psi*
p_D	*Dimensionless pressure*
p_{wf}	*Flowing bottom hole pressure, psi*
p_{ws}	*Shut-in bottom hole pressure, psi*
q	*Well head flow rate, STB/D*
q_f	*Bottom hole flow rate, STB/D*
r	*Distance from well, ft*
r_D	*Dimensionless distance*
r_i	*Radius of investigation, ft*
r_s	*Real skin radius, ft*
r_w	*Well bore radius, ft*
s	*near wellbore skin factor*
t	*Time, hrs*
t_p	*production time, hrs*
t_D	*Dimensionless time*
T	*Temperature, °F*
V_w	*Volume of the well, ft³*
Z	*Gas compressibility factor, dimensionless*
P	*Pressure difference, psi*
ΔP_s	*Pressure drop due to skin, psi*
Z_W	*Vertical coordinate of center of horizontal well, ft*
L	*Horizontal well length, ft*
Δt	*Time interval, hrs*
Δt_e	*Equivalent time, hrs*
μ	*Viscosity, cp*
ρ	*Density, lb/ft³*
ω	*Storage coefficient, fraction*
α	*Characteristic factor for NFR, 1/ft²*
λ	*Interporosity flow parameter, fraction*
Φ	*porosity, fraction*

References

[1] Haykin S. Neural networks: A comprehensive foundation, 2004; 2: 41-53.

[2] Al-Kaabi A, Lee W. An artificial neural network approach to identify the well test interpretation model: applications, SPE annual technical conference and exhibition, Society of Petroleum Engineers, 1990.

[3] Alajmi M.N, Ertekin T. The development of an artificial neural network as a pressure transient analysis tool for applications in double-porosity reservoirs, Asia Pacific oil and gas conference and exhibition, Society of Petroleum Engineers, 2007.

[4] Allain O, Houze O. A practical artificial intelligence application in well test interpretation, European petroleum computer conference, Society of Petroleum Engineers, 1992.

[5] Adibifard M, Tabatabaei-Nejad S, Khodapanah E. Artificial Neural Network (ANN) to estimate reservoir parameters in Naturally Fractured Reservoirs using well test data. Journal of Petroleum Science and Engineering, 2014; 122: 585-594.

[6] Shahbazi K, Zarei AH, Shahbazi A, Tanha AA. Investigation of production depletion rate effect on the near-wellbore stresses in the two Iranian southwest oilfields. Petroleum Research, 2020; 5: 347-361.

[7] Yasin IBE. Pressure transient analysis using generated well test data from simulation of selected wells in norne field. Institute For Petroleum Technology of Anvendt Geofysik, 2012.

[8] Behmanesh H, Hamdi H, Clarkson C, Thompson J, Anderson D, Chin A. Transient linear flow analysis of multi-fractured horizontal wells considering three-phase flow and pressure-dependent rock properties. Unconventional Resources Technology Conference, Houston, Texas, 23-25 July 2018, Society of Exploration Geophysicists, American Association of Petroleum, 2018; 1634-1653.

[9] Chen Z, Liao X, Zhao X, Dou X, Zhu L. Performance of horizontal wells with fracture networks in shale gas formation. Journal of Petroleum Science and Engineering, 2015; 133: 646-664.

[10] Bahrami N, Pena D, Lusted I, Well test, rate transient analysis and reservoir simulation for characterizing multi-fractured unconventional oil and gas reservoirs. Journal of Petroleum Exploration and Production Technology, 2016; 6: 675-689.

[11] Kuchuk F, Morton K, Biryukov D. Rate-transient analysis for multistage fractured horizontal wells in conventional and un-conventional homogeneous and naturally fractured reservoirs. SPE Annual Technical Conference and Exhibition, Society of Petroleum Engineers, 2016.

[12] Zargar G, Tanha AA, Parizad A, Amouri M, Bagheri H. Reservoir rock properties estimation based on conventional and NMR log data using ANN-Cuckoo: A case study in one of super fields in Iran southwest. Petroleum, 2020; 6: 304-310.

[13] Zhang M, Ayala LF. Application of superposition principle to variable rate/pressure production analysis of multi-fractured horizontal wells in unconventional gas reservoirs. Journal of Natural Gas Science and Engineering, 2019;72: 103-111.

[14] Serra K, Reynolds A, Raghavan R. New pressure transient analysis methods for naturally fractured reservoirs (includes associated papers 12940 and 13014). Journal of Petroleum Technology, 1983; 35: 271-283.

[15] He Y, Cheng S, Rui Z, Qin J, Fu L, Shi J, Wang Y, Li D, Patil S, Yu H. An improved rate-transient analysis model of multi-fractured horizontal wells with non-uniform hydraulic fracture properties. Energies, 2018; 11: 393-404.

[16] He y, Qin j, Cheng S, Chen J. Estimation of fracture production and water breakthrough locations of multi-stage fractured horizontal wells combining pressure-transient analysis and electrical resistance tomography. Journal of Petroleum Science and Engineering, 2020; 194: 107-119.

[17] Meng M, Chen Z, Liao X, Wang J, Shi L. A well-testing method for parameter evaluation of multiple fractured horizontal wells with non-uniform fractures in shale oil reservoirs. Advances in Geo-Energy Research, 2020; 4: 187-198.

[18] Larki E, Tanha AA, Parizad A, Soulgani BS, Bagheri H. Investigation of quality factor frequency content in vertical seismic profile for gas reservoirs. Petroleum Research, 2021; 6: 57-65.

[19] Qin J, Cheng S, He Y, Wang Y, Feng D, Yang Z, Li D, Yu H. Decline curve analysis of fractured horizontal wells through segmented fracture model. Journal of Energy Resources Technology, 2019; 141: 305-314.

[20] Wu Y, Cheng L, Huang S, Jia P, Zhang J, Lan X, Huang H. A practical method for production data analysis from multistage fractured horizontal wells in shale gas reservoirs. Fuel, 2016; 186: 821-829.
[21] Zeng J, Wang X, Guo J, Zeng F. Composite linear flow model for multi-fractured horizontal wells in heterogeneous shale reservoir. Journal of Natural Gas Science and Engineering, 2017; 38: 527-548.
[22] Zhao Y, Zhang L, Xiong Y, Zhou Y, Liu Q, Chen D. Pressure response and production performance for multi-fractured horizontal wells with complex seepage mechanism in box-shaped shale gas reservoir. Journal of Natural Gas Science and Engineering, 2016; 32: 66-80.
[23] Deng Y, Chen Q, Wang J. The artificial neural network method of well-test interpretation model identification and parameter estimation. International Oil and Gas Conference and Exhibition in China, Society of Petroleum Engineers, 2000.
[24] Lu J, Zhu T, Tiab D. Pressure behavior of horizontal wells in dual-porosity, dual-permeability naturally fractured reservoirs. SPE Middle East Oil and Gas Show and Conference, Society of Petroleum Engineers, 2009.
[25] Stehfest H. Numerical inversion of Laplace transforms . Communications of the ACM, 1970; 13: 47-49.
[26] Zhao X, Rui Z, Liao X, Zhang R. A simulation method for modified isochronal well testing to determine shale gas well productivity. Journal of Natural Gas Science and Engineering, 2015; 27: 479-485.
[27] Wang Y, Yi X. Flow modeling of well test analysis for a multiple-fractured horizontal well in triple media carbonate reservoir. International Journal of Nonlinear Sciences and Numerical Simulation, 2018; 19: 439-457.
[28] Zeng J, Wang X, Guo J, Zeng F, Zhang Q. Composite linear flow model for multi-fractured horizontal wells in tight sand reservoirs with the threshold pressure gradient. Journal of Petroleum Science and Engineering, 2018; 165: 890-912.
[29] Dejam M, Hassanzadeh H, Chen Z. Semi-analytical solutions for a partially penetrated well with wellbore storage and skin effects in a double-porosity system with a gas cap. Transport in porous media, 2013; 100: 159-192.

To whom correspondence should be addressed: Dr. Abbas Ayatizadeh Tanha, Ahwaz Faculty of Engineering, Petroleum University of Technology, Iran; e-mail: a.ayatizadeh@modares.ac.ir
Ghassem Zargar, *Ahwaz Faculty of Engineering, Petroleum University of Technology, Iran, e-mail: zargar@put.ac.ir*